Capillary Extrusion Behavior of Phenolphthalein Poly(ether-ether-sulphone) (PES-C)

YINGWEI DI,[1] DOMENICO ACIERNO,[2] ALBERTO D'AMORE,[3] ROSSELLA NOBILE,[2] LUIGI NICOLAIS[3]

[1] Department of Chemistry, Northeast Normal University, 138 People Street, Changchun 130024, People's Republic of China

[2] Department of Chemical and Food Engineering, University of Salerno, Fisciano (SA), Italy

[3] Department of Materials and Production Engineering, University of Napoli, Napoli, Italy

Received 20 June 1996; accepted 10 December 1996

ABSTRACT: The capillary extrusion flow properties of novel engineering thermoplastic phenolphthalein poly(ether-ether-sulphone) (PES-C) have been investigated using capillary rheometer. The dependence of viscosity on the wall shear rate and temperatures were obtained. The flow activation energy was found to decrease with shear rate but to be constant with shear stress. The entrance effect was calculated and from which the extensional behavior was estimated using Cogswell's method. From the extrudate swell ratio the principal normal stress was evaluated and a temperature-independent correlation was observed when they were plotted against shear stress. The melt fracture phenomena were checked and discussed also. © 1997 John Wiley & Sons, Inc. J Appl Polym Sci **65:** 951–958, 1997

Key words: phenolphthalein poly(ether-ether-sulphone)(PES-C); capillary flow; entrance pressure drop; extrudate swell; melt fracture

INTRODUCTION

As there have been increasing demands in engineering thermoplastics for high temperature applications, several excellent thermoplastics have been developed in the last 2 decades such as PEEK, PES, and PEI. Phenolphthalein poly(ether-ether-sulphone) PES-C, as a new emerging member of the family of engineering thermoplastics, has become more and more applicable in many fields including as a matrix of the advanced composites used at elevated temperatures, as it was developed in the last decade,[1] because of its high-temperature resistance ($T_g \approx 245°C$), excellent mechanical properties whose tensile strength is more than 100 MPa at room temperature, better solubility in certain solvents, and more economical cost. Owing to the cardo group attached on its main chain, it is an amorphous polymer with exceptional thermal stability. Being a new system of polymer and also due to its thermoplastic nature, an understanding of the melt rheology of PES-C is essential for both industrial and academic interests in optimizing and determining the proper processing conditions.

It has been known that pressure-driven flow through tubes and other types of channels are of central importance in experimental rheology and in polymer processing. Not only is this flow used as the basis for the most popular type of melt rheometer, but it is also a flow that occurs often in melt processing, for example, in an extrusion die or in the runner feeding an injection mold. In this study the capillary rheometer, which can stimulate the melt flow behavior in the important processing operations aforementioned, was used

Correspondence to: Y. Di.

 CCC 0021-8995/97/050951-08

to study the extrusion properties of PES-C melts at its processing temperatures. Here we present the results of the investigation of the capillary flow properties on PES-C melt including flow curves, temperature effect, entrance effect, extrudate swell, and melt fracture.

EXPERIMENTAL

Materials

Phenolphthalein poly(ether-ether-sulphone) (PES-C) is now commercially available in China. The sample used here were supplied by Xuzhou Engineering Plastics Co. in the form of a powder, with the reduced viscosity of 0.45 in chloroform at 25°C, corresponding M_w of 7.3×10^5 kg/mol, and MWD of 1.96, and its chemical structure is as follows:

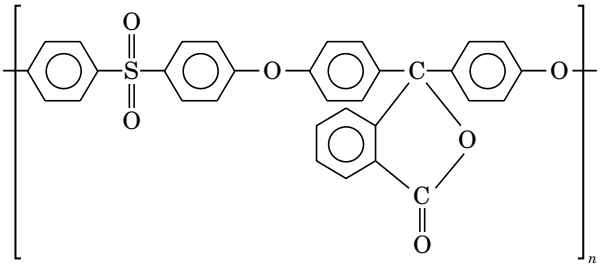

Sample Preparation

The powder materials were extruded twice and pelletized using a twin-screw extruder with an L/D of 22 and a compression ratio of 23 under conditions of cylinder and die temperature of 320, 330, 340, and 340°C with screw revolution speeds of 40 rpm. Before extrusion, the materials were dried in a vacuum oven at 140°C overnight to erase any moisture and solvent residuals. The reduced viscosity of extrudates was measured again after extrusion and the molecular weight changes were found to be insignificant.

Capillary Characterization

Melt rheology, die swell, and melt fracture were investigated using the CEAST capillary rheometer, Rheoscope 1000, in which the flow of the sample is generated by a piston moving down at constant speed in a reservoir above the capillary. The reservoir has a dimension of 9.5 mm diameter and 166 mm length. The samples in the form of pellets were dried in a vacuum oven at 120°C overnight before being loaded into the rheometer. All flat dies used for the rheology study had a diameter of 1 mm, and three different dies of length-to-diameter ratios (L/D) of 5, 10, and 20 were used in this study. The experimental temperature for extrusion is controlled by the heating sheath around the reservoir, and temperatures of 330, 340, 350, and 360°C were used in this study. The piston speeds vary from 0.5–50 mm/min, as showed in Table I. The drive pressure (P) was measured at the top of the piston and the volumetric flow rate (Q) was directly calculated as a product of the set piston speed and cross-sectional area of the barrel. Their values obtained before the appearance of melt fracture were used to determine the flow curves.

Ideal extrudate swell measurements should be performed under the following conditions[2]: steady isothermal flow, absence of gravitation force as well as interfacial tension, and should be in a state of complete elastic recovery. There are several methods of measurement of extrudate swell.[2–4] In this study the simplest method was adopted, i.e., quenching the extrudates in air after they were extruded from the capillary, and then measuring their diameters at a constant distance of 2 cm from the exit of the capillary at room temperature using a micrometer when they were air frozen. The diameter of the extrudate, D, was determined as an average of two measurements at right angles to each other (or as nearly as possible). This was done to compensate for the noncircular cross-sections and each time at least five samples were used and averaged to get the value of D. The ratio D/D_0, where D_0 is the capillary diameter, was called die swell ratio and used as a measure of extrudate swell.

Onset of melt fracture was simply determined by the observation of the extrudates appearance with naked eye, and the occurrence of melt fracture was checked.

RESULTS AND DISCUSSION

Flow Curves

The apparent shear stress τ_a and the apparent shear rate $\dot{\gamma}_a$ at the wall in capillary flow are given by following two equations:[5]

$$\tau_a = \frac{P \cdot D}{4L} \tag{1}$$

Table I The Melt Flow Indexes for PES-C as a Function of Apparent Shear Rate

Piston Speed (mm/min)	Apparent Shear Rate (l/s)	360°C	350°C	340°C	330°C
0.5	6.02	0.94	0.93	0.761	0.712
1	12.03	0.876	0.845	0.707	0.655
2	24.04	0.813	0.76	0.653	0.599
5	60.2	0.728	0.648	0.583	0.524
10	120.3	0.665	0.563	0.529	0.468
20	240.4	0.601	0.478	0.476	—
50	602	0.517	0.366	—	—

$$\dot{\gamma}_a = \frac{32Q}{\pi D^3}, \qquad (2)$$

where P and Q are pressure dropped through the capillary and the volumetric flow rate of melt from the capillary. Figure 1 shows, as an example, the apparent flow curves ($\dot{\gamma}_a - \tau_a$) obtained directly from eqs. (1) and (2) for the data at 360°C with different dies.

Due to the entrance pressure loss, the apparent flow curve obtained with a die of a smaller L/D locates at a higher shear stress side (Fig. 1). To obtain real stress at the wall of capillary, τ_w, the Bagley end correction is often adopted[5]:

$$\tau_w = \frac{P}{2\left(\frac{2L}{D} + e\right)} = \frac{P - P_{\text{ent}}}{4\,L/D}, \qquad (3)$$

where e is the end correction and P_{ent} is the entrance pressure drop. Either of them can be calculated as the respective intercept of L/R and P axes by extrapolating the straight lines of P vs. L/D (Bagley plot), which are plotted at a definite apparent shear rate $\dot{\gamma}_a$, to the P = 0 axis. Fine Bagley plots were obtained for all samples, and an example of these plots is shown in Figure 2 for PES-C at 360°C. The flow curve ($\dot{\gamma}_a - \tau_w$) at 360°C by correcting the apparent shear stress τ_a to the effective wall shear stress τ_w using eq. (3) can be obtained, and each flow curve with a different L/D unites into one curve, independent of L/D (for the reason of clarity, they are not shown in Fig. 1).

On the other hand, the non-Newtonianity of flow is also needed to be corrected and "the Rabinowitch correction"[5] is usually used by feeding back the entrance correction into the data to get the plots of log (wall shear stress, τ_w) vs. log (apparent shear rate, $\dot{\gamma}_a$). The slopes of these later plots,

$$n = \frac{d \log \tau_w}{d \log \dot{\gamma}_a},$$

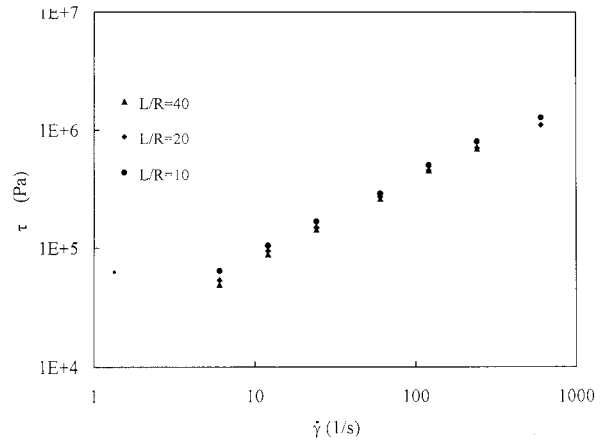

Figure 1 The apparent shear stress vs. the apparent shear rate for for PES-C at 360°C.

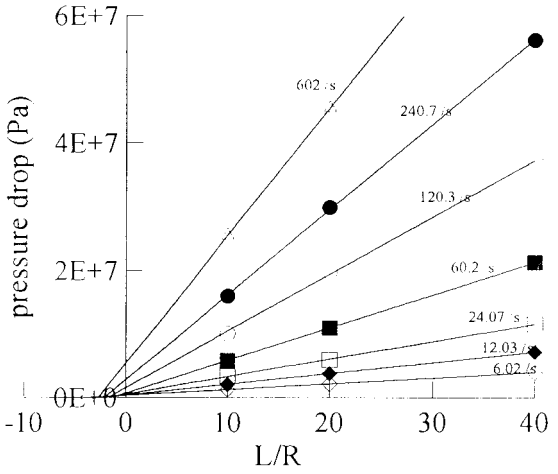

Figure 2 The Bagley entrance correction plot for PES-C at 360°C.

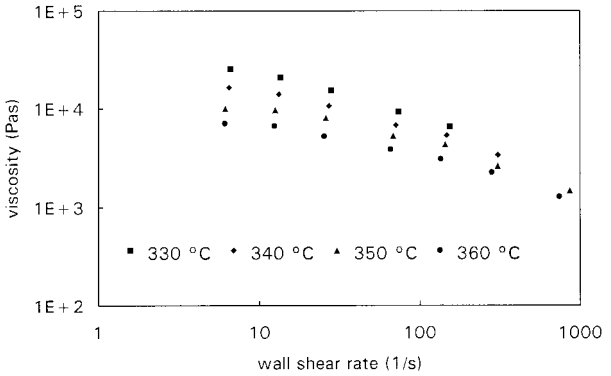

Figure 3 The capillary flow curves for PES-C at four temperatures.

which are called the polymer flow behavior index at various temperatures, were calculated by the regression analysis and the wall shear rates, $\dot{\gamma}_w$, were given as follows:

$$\dot{\gamma}_w = \left(\frac{3n + 1}{4n}\right) \cdot \dot{\gamma}_a. \tag{4}$$

By referring to Figure 3, the data do not fall on a straight line, which implies that the melt behavior of PES-C is neither Newtonian nor power-law, and n will change with shear rate at each temperature. Consequently, the values of n have been calculated by the nonlinear regression analysis on the experimental log $\dot{\gamma}_a$ vs. log τ_w plot and are shown in Table I. Non-Newtonian pseudoplastic fluids are characteristic of n below 1. Therefore, a high value of n indicates a low pseudoplastic or non-Newtonian nature of the polymer melt. From Table I we can observe that at each apparent shear rate the values of n increase with temperature, and at each temperature they decrease with the shear rate, which indicates that the melt behavior of PES-C becomes more and more pseudoplastic as temperature decreases and shear rate increases.

The true flow curve ($\dot{\gamma}_w - \tau_w$) after correcting the apparent shear rate $\dot{\gamma}_a$ to the wall shear rate $\dot{\gamma}_w$ using eq. (4) can be obtained, and in this manner the true flow curves of the sample at various temperatures were obtained and shown in Figure 3 by plotting η vs. $\dot{\gamma}_w$, in which the more clearly shear-thinning behavior than plotting $\dot{\gamma}_w$ against τ_w is shown.

In Figure 3 it is showed that increased shearing decreases the melt viscosity as expected like other high performance thermoplastics polymeric materials, for example, Victrex 380 PEEK[6] and PES[7], which all show the shear-thinning behavior. Because no significant molecular weight changes were detected after extrusion, the shear-thinning behavior of the melt must therefore be due to changes in melt morphology. It has been plausibly postulated[8,9] that shear modification reduces the number of entanglements in the melt and, therefore, results in the shear-thinning behavior.

Temperature Dependence

The temperature dependence of the viscosity of polymer melts at temperatures above T_g + 100°C or so can be expressed by the flow activation energy, E_a, as following:

$$\eta = A \cdot \exp(E_a/RT) \tag{5}$$

where A is a constant parameter independent of temperature. Figure 4 is an Arrhenius type plot showing viscosity temperature dependence of PES-C melt at two constant shear stresses and two constant shear rates, respectively. The flow activation energy calculated from these plots are given in Table II. Because the flow behavior of the polymer melt is dependent upon the shear rate and temperature, the flow activation energy of a polymer melt evaluated in the non-Newtonian region at a constant shear rate will vary with the shear rate chosen, as shown in Table II, which with the increase of shear rate, the activation energy will decrease. The higher the flow activation energy, the more temperature sensitive is the melt. So like other polymers, the temperature dependence of PES-C melts will get weak when increasing the shear rate. On the other hand, the activation energies calculated at constant shear

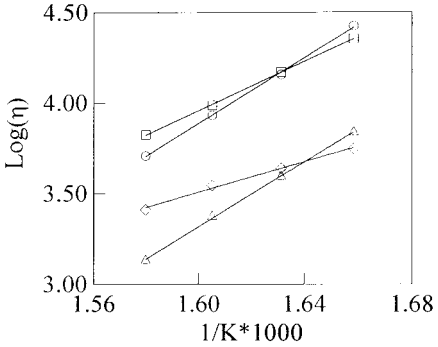

Figure 4 The temperature dependence of the viscosity for PES-C at two constant shear stresses and two shear rates, respectively.

Table II The Flow Activation Energy for PES-C at Two Constant Shear Stresses and Two Constant Shear Rates

	τ_1 = 1.6E5 Pa	τ_2 = 9.6E5 Pa	$\dot{\gamma}_1$ = 10 s^{-1}	$\dot{\gamma}_2$ = 200 s^{-1}
E_a (kJ/mol)	171	173	130	81

stresses vary little. So activation energy calculated in this way is more important in understanding the temperature dependence than that evaluated at constant shear rates.[10] For some other polymers, for example, PVC, when the flow activation energy has been evaluated at a constant shear rate, the existence of two types of flow has been reported by Collins[11] et al. At constant shear stress, there was only slight evidence to such a flow behavior. This is called transitional flow behavior. The transition point varies with molecular weight, temperature, shear stress, or shear rate. From our results shown in Figure 4, little changes of activation energy at each constant shear stress were observed, i.e., we could not observe the existence of a two-type flow behavior from the Arrhenius plots made at constant shear stress in the temperature range used in this study. However, the flow activation energy evaluated at different shear rates did change with the shear rate. The reduction in flow activation energy obviously resulted from the highly non-Newtonian behavior of the PES-C melt in high shear rate range, as shown by the melt flow indexes, n, in Table I.

Entrance Effect

The entrance pressure drop values, P_{ent}, from Bagley plots, i.e., plots of P vs. L/R at fixed shear rate, are determined by simple linear least-square fitting, as shown in Figure 2. The results are shown in Figure 5, where the variation of the entrance pressure drop with apparent shear rate $\dot{\gamma}_a$ at different temperatures can be observed. P_{ent} increases with increasing $\dot{\gamma}_a$ and decreases with increasing temperature. A large pressure drop at the capillary entrance for polymer melts, compared to that for Newtonian fluids, has been almost exclusively attributed to the elasticity of polymer melts.[12] Therefore, it can be said here that the melt elasticity of PES-C decreases with the increase of temperature. The contribution of P_{ent} to the total pressure drop varies with the dies. For the smallest L/R die (L/R = 10) the entrance effects account for 31.7% of the total pressure drop, while for the largest (L/R = 40) it is only 10.9% at a temperature of 360°C and apparent shear rate of 60.2 s^{-1}. So P_{ent} is a important parameter characterizing the materials elastic properties.

Because of the high degree of tensile extension (stretching along streamline) that occurs at the entrance, which also causes the entrance pressure loss, the entrance pressure drops are also required when using the method of Cogswell[13] to assess the extensional behavior of the melt. These equations are derived from a simple geometric analysis. In this analysis it is assumed that the pressure drop has two components—one due to shear and one to extension—and with a further assumption that the extensional strain is sufficiently large that the stored elastic energy resulting from stretching is approximately equal everywhere to some maximum value. The estimated apparent extensional strain rate is thus given by:

$$\dot{\varepsilon}_E = \frac{4\dot{\gamma}_a^2 \cdot \eta_a}{3(n+1)P_{ent}}, \qquad (6)$$

where $\dot{\gamma}_a$ is the apparent shear rate given in eq. (2) and n is the flow behavior index as shown in Table I. The apparent extensional stress is given by:

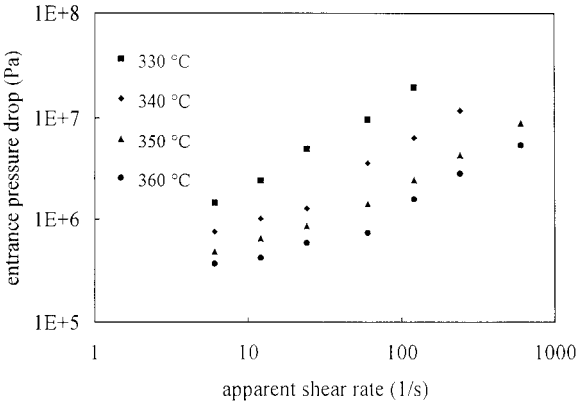

Figure 5 The entrance pressure drop for PES-C at different temperatures as a function of the shear rate.

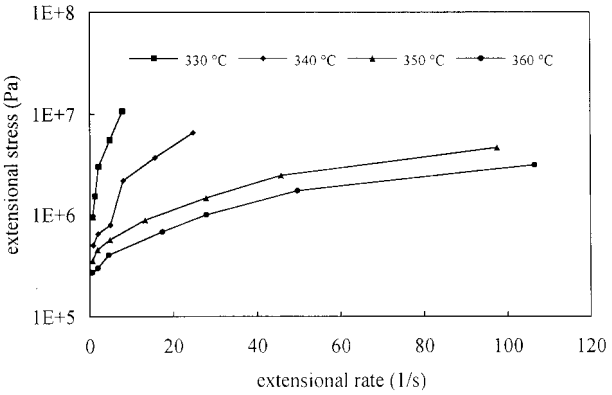

Figure 6 The extensional stress vs. extensional rate for PES-C at different temperatures.

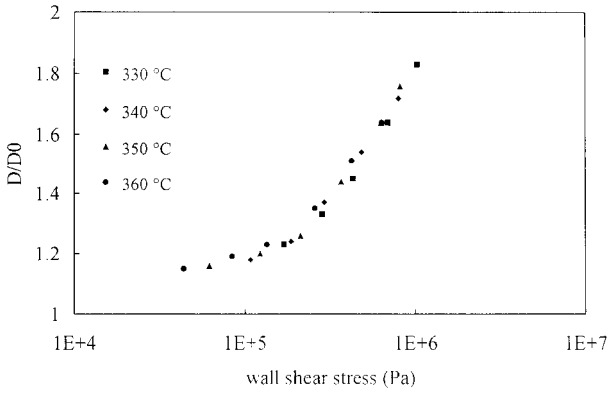

Figure 7 The extrudate swell ratio vs. wall shear stress for PES-C at different temperatures.

$$\sigma_E = \frac{3}{8}(n + 1)\Delta P_{\text{ent}}. \tag{7}$$

Thus, we see that

$$\eta_E = \frac{9(n + 1)^2(P_{\text{ent}})^2}{32\eta_a\dot{\gamma}_a^2} = \frac{\eta_a}{2}\left[\frac{\dot{\gamma}_a}{\dot{\varepsilon}}\right]^2. \tag{8}$$

The results for the PES-C used in this study are shown in Figure 6. It can observed that the extensional stress is an increasing function of the extensional strain rate like the steady shear behavior showed before. This also agrees with the behavior described by others[14] for application of Cogswell's method to the other polymers. There has also been a report[15] on the agreement between the values of η_E calculated from this equation for several polymers and the true extensional viscosity determined using elaborate extensional rheometers; however, this agreement only covered narrow ranges of strain rate, and for some other exceptional resins and strain rate there was no quantitative correlation between the two functions. So we could only conclude intuitively here that Figure 6 at least showed the general and qualitative trend of extensional behavior for PES-C.

Extrudate Swell

The die swell ratio is defined as the value of extrudate diameter divided by the value of die diameter. Figure 7 shows the variation of die swell ratio D/D_0 with wall shear stress τ_w using temperature as a parameter. For the Newtonian fluid the ratio is about 1.13,[16] but for PES-C they are larger than that. These large swell ratios are a manifestation of the molecular orientation that is generated by the flow in the die. In general, the die swell ratios of thermoplastic resins increase monotonously with increasing shear rate or shear stress. But there are also exceptions, for example, poly(vinyl chloride), whose variation of the die swell ratio with shear rate sometimes shows a maximum or a minimum.[12] It can be observed that for PES-C melt it follows the general trend and gives rise to a temperature-independent correlation when its D/D_0 are plotted against τ_w for PES-C. This temperature independence has been reported for several polymer melts.[17] Increasing the length-to-diameter ratio the melt swell is reduced, as shown in Figure 8. It is because as the melt gets into the capillary from the entrance region, relaxation of the molecular chain will lead to a loss of the orien-

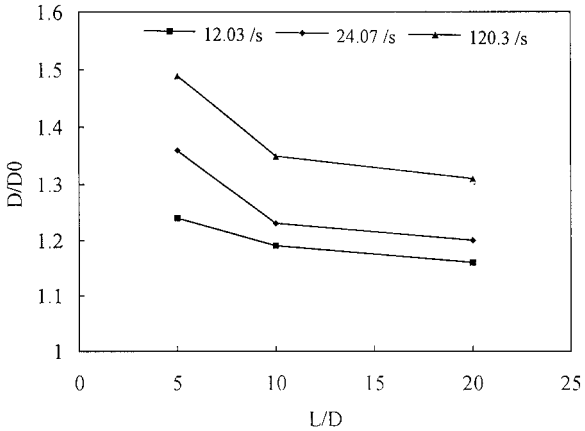

Figure 8 The variation of extrudate swell with the die geometry for PES-C at 360°C.

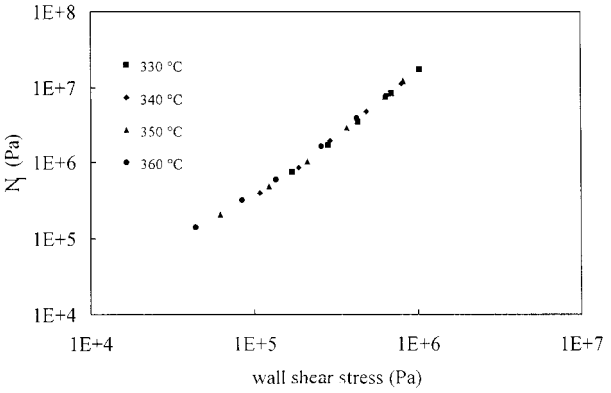

Figure 9 The principal normal stress differences plot for PES-C at different temperatures.

tation generated at the entrance region. So, as the capillary is lengthened, the degree of swell is reduced.

The principal normal stress difference ($\tau_{11}-\tau_{22}$) is also a parameter characterizing the elasticity of polymer melts. In this study, the principle normal stress differences were calculated from the die swell ratio and wall shear stress according to Tanner's equation[18]:

$$\tau_{11}-\tau_{22} = 2\tau_w[2(D/D_0)^6 - 2]^{1/2}. \qquad (9)$$

The calculated principal normal stress difference as a function of shear stress are shown in Figure 9, revealing that the $\tau_{11}-\tau_{22}$ of PES-C increases with shear stress and are independent of temperature, very similar to the temperature independence of the extrudate swell. Similar results have also been reported for some other polymers and the dispersed multiphase polymer melts,[17] in which the $\tau_{11}-\tau_{22}$ were measured directly by using Weissenberg Rheogoniometer in the low shear rate range. Because the principal normal stress difference could only be measured precisely with the cone/plate rotational rheometer, which is limited in low shear rate range and measurement in high shear rate range becomes experimentally difficult. So the results we obtained here at the high shear rate range according to the empirical equation are more useful for actual processing design.

Melt Fracture

Melt fractures occurred at each experiment with different die and temperatures were checked with the naked eye, and the rheological data analyzed in this study were all obtained when they started. The experimental observation showed that the melt fractures in this study had the appearance of a helical screw thread. It has been suggested[19] that this type of distortion results from the abrupt change in the boundary condition at the exit of the die, which causes a high degree of stretching in the surface layer of the melt as it leaves the die. This stretching produces tensile stresses that can exceed the strength of the melt, leading to surface fracture. But later careful studies[20] of extrudates of linear polyethylene also suggest that the onset of this surface fracture is accompanied by the occurrence of wall slip in the capillary. In our experiment, when the fracture phenomena occurred, the oscillation of the pressure were observed, which is the reflection of the melt slip on the capillary wall. Thus, this type of distortion is clearly an exit effect and it may be also associated with the slip flow in the capillary.

Melt fractures often occur at a critical shear stress or a critical shear rate, depending on the different dies. In this study, the critical shear stress was recorded as the onset of noticeable melt fracture occurs, and they were found varied with temperature. Much higher shear rates in Figure 3 at different temperatures were hindered by the melt fracture. A further study on the melt fracture phenomena of PES-C is in progress.

CONCLUSION

The extrusion flow properties of the novel engineering thermoplastic PES-C have been investigated using a capillary rheometer. It showed a similar pseudoplastic behavior as the other engineering thermoplastics, for example, PEEK and PES, and by rough comparison with the data in refs. 6 and 7 on PEEK and PES, we can observe that the viscosity values of PEEK and PES at 350°C are in the same order of magnitude as that of PES-C at 350°C in the same shear rate range. So the material used in this study also exhibits high viscosity like other high-performance thermoplastics. Efforts of reducing its processing viscosity without losing its mechanical properties should also be considered in their processing. The flow activation energy of PES-C did not change significantly with shear stress, and decreased with the increasing of the shear rate. The entrance pressure drop at different dies increased as the temperature decreased , and the extensional behavior was estimated for them. The die swell

ratios D/D_0 of the melts increased with shear stress and decreased with the length-to-diameter ratio. The principal normal stress at high shear rate were evaluated using Tanner's equation. Because both the principle normal stress difference and extrudate swell (i.e., the energy stored) are increased as temperature is decreased as well as the shear stress (i.e., the energy dissipated), we can conclude from our experimental observations that temperature seems to have little effect on the ratio of the principle normal stress difference to the shear stress and that of the extrudate swell to shear stress for the PES-C melt. The melt fractures showed the appearance of a helical screw thread. The critical shear stress were found to change with both dies and temperature, and they are the hindrance for high shear rate or stress application of the PES-C melt in the capillary test.

REFERENCES

1. K. Liu, H. Zhang, and T. Chen, Chinese pat. 85101721 (1985).
2. L. A. Utraki, Z. Bakerdjian, and M. R. Kamal, *J. Appl. Polym. Sci.,* **19,** 48 (1975).
3. W. M. Graessley, S. D. Glasscock, and R. L. Grawley, *Trans. Soc. Rheol.,* **14,** 4 (1970).
4. C. D. Han and T.C. Yu, *AIChE J.,* **17,** 1512 (1971).
5. M. J. Dealy and K. F. Wissbrun, *Melt Rheology and Its Role in Plastics Processing,* Van Nostrand Reinhold (VNR), New York, 1990.
6. A. Mehta and A. I. Isayev, *Polym. Eng. Sci.,* **31,** 971 (1991).
7. S. G. James, A. M. Donald, and W. A. MacDonald, *Mol. Cryst. Liq. Cryst.,* **153,** 501 (1987).
8. A. Rudin and H. P. Schreiber, *Polym. Eng. Sci.,* **23,** 422 (1983).
9. P. J. R. Lebans and C. Bastiaansen, *Macromolecules,* **22,** 3322 (1989).
10. R. S. Porter, J. Whan, and F. Johnson, *J. Polym. Sci.,* **C15,** 365 (1966).
11. E. A. Collins and C. A. Krier, *Trans. Soc. Rheol.,* **11,** 225 (1967).
12. M. Fujiyama and Y. Kawasaki, *J. Appl. Polym. Sci.,* **42,** 467 (1991).
13. F. N. Cogswell, *Polym. Eng. Sci.,* **12,** 64 (1972).
14. A. J. Muller, V. Balsamo, F. Da Silva, C. M. Rosoles, and A. E. Saez, *Polym. Eng. Sci.,* **34,** 1455 (1994).
15. H. M. Laun and H. Schuch, *J. Rheol.,* **33,** 119 (1989).
16. K. Reddy and R. I. Tanner, *J. Rheol.,* **22,** 661 (1978).
17. K. J. Wang and L. J. Lee, *J. Appl. Polym. Sci.,* **33,** 431 (1987).
18. R. I. Tanner, *J. Polym. Sci., A-2,* **14,** 2067 (1970).
19. N. F. Cogswell, *Polymer Melt Rheology,* John Wiley & Sons, New York, 1981, p. 101.
20. D. S. Kalida and M. M Denn, *J. Rheol.,* **31,** 815 (1987).